Structural and superconducting properties of $Bi_{1.7}Pb_{0.4}Sr_{2-x}Yb_xCa_{1.1}Cu_{2.1}O_y$ system

A. Biju, R.P. Aloysius, U. Syamaprasad *

Regional Research Laboratory (CSIR), Trivandrum-695019, India

Abstract

The structural, electrical and superconducting properties of $Bi_{1.7}Pb_{0.4}Sr_{2-x}Yb_xCa_{1.1}Cu_{2.1}O_y$ system has been studied for different Yb concentrations. The samples are prepared by solid state synthesis in the polycrystalline bulk form. Structural analysis by X-ray diffraction, microstructural examination by SEM and measurements of electrical and superconducting properties have been conducted to study the effects of Yb substitution at Sr site. The critical temperature (T_C) and critical current density (J_C) are found to increase drastically with Yb substitution. Maximum values of T_C and J_C are observed for $x=0.3$ and $x=0.2$ respectively. The increase in T_C and J_C is explained due to the substitution effect of Yb^{3+} in place of Sr^{2+} and consequent change in the hole concentration in the CuO_2 planes. Above the optimum levels T_C and J_C begin to reduce due to secondary phase formation. A metal–insulator transition originating from the change of carrier concentration is found to occur at higher doping level ($x>0.5$).
© 2006 Elsevier B.V. All rights reserved.

1. Introduction

Copper oxide based superconductors need an optimum carrier concentration for the occurrence of superconductivity, below which the material turns into the insulating regime. Cationic substitution at different sites in a cuprate superconducting system leads to changes in carrier concentration and effect of such changes is one of the important features that helps in understanding the superconducting properties and structural details of the system along with the understanding of the fundamental mechanism of the occurrence of superconductivity [1–3]. In Bi-based superconducting systems variations in hole concentration of the CuO_2 planes can be achieved by cationic substitution of the divalent Ca/Sr by trivalent rare earth elements. Recent studies on the substitution of rare earths in the Bi-based superconductors [2,3] have shown that cation disorders in particular that located at Sr site significantly affect the T_C of the system. Moreover the crystal structure of the parent system remains invariant with these substitution even though a significant change in the carrier concentration occurs due to cation doping.

Among the Bi-based superconducting systems, Bi-2212 has advantages with respect to its thermodynamic and structural stability against relatively large variations in processing conditions as well as on different cationic substitutions made on the parent system. For example there are numerous reports on the improvement of T_C and J_C of this system by different cationic substitutions at different sites [4–22] including rare earth elements.

Among the rare earth elements, there are reports on the substitution on Yb for Ca [5–8] in varying amounts in the parent system having a stoichiometry of $Bi_2Sr_2Ca_{1-x}Yb_xCu_2O_y$. As far as superconducting properties are concerned an Yb stoichiometry of $x=0.2–0.25$ is found to be optimum, yielding higher T_C and reduced amount of secondary phases. More over most of the rare earths have been substituted at Ca site on the general formula $Bi_2Sr_2Ca_{1-x}RE_xCu_2O_y$[RE: Rare Earth]. In this paper

---

* Corresponding author. Tel.: +91 471 2515373; fax: +91 471 2491712.
E-mail address: syam@csrrltrd.ren.nic.in (U. Syamaprasad).

we report the effect of substitution of Yb, a rare earth element by varying the Sr stoichiometry on the general formula of $Bi_2Sr_{2-x}RE_xCa_1Cu_2O_y$.

2. Experimental details

(Bi, Pb)-2212 superconductor having a general stoichiometry of $Bi_{1.7}Pb_{0.4}Sr_{2-x}Yb_xCa_{1.1}Cu_{2.1}O_y$. (where $x=0$, 0.1, 0.2, 0.3, 0.4, 0.5, 0.7 and 0.9) were prepared by solid state synthesis route using high purity chemicals Bi_2O_3, PbO, $SrCO_3$, $CaCO_3$, CuO and Yb_2O_3 (Aldrich, >99.9%). The stoichiometric amounts of the ingredients were weighed using an electronic balance (Mettler AE 240), thoroughly mixed and ground using an agate mortar and pestle. The samples were then subjected to a three stage calcination process in air at different temperatures of 800 °C/15 h, 820 °C/20 h, and 840 °C/40 h, with a heating rate of 3 °C/min. Intermediate grinding was done between each stage of calcination. After calcination the samples were pelletized using a cylindrical die of 12 mm diameter under a force of 60 kN. All the pellets were then heat treated at 845 °C for 100 h (50 + 50) in two stages with one intermediate pressing at the same force. The final thickness of the pellets was ~ 1 mm.

Phase analyses of the samples were done using XRD (Philips *X'pert Pro*) employing X'celerator and monochromator at the diffracted beam side. Phase identification was performed using *X'Pert* High score software in support with ICDD-PDF 2
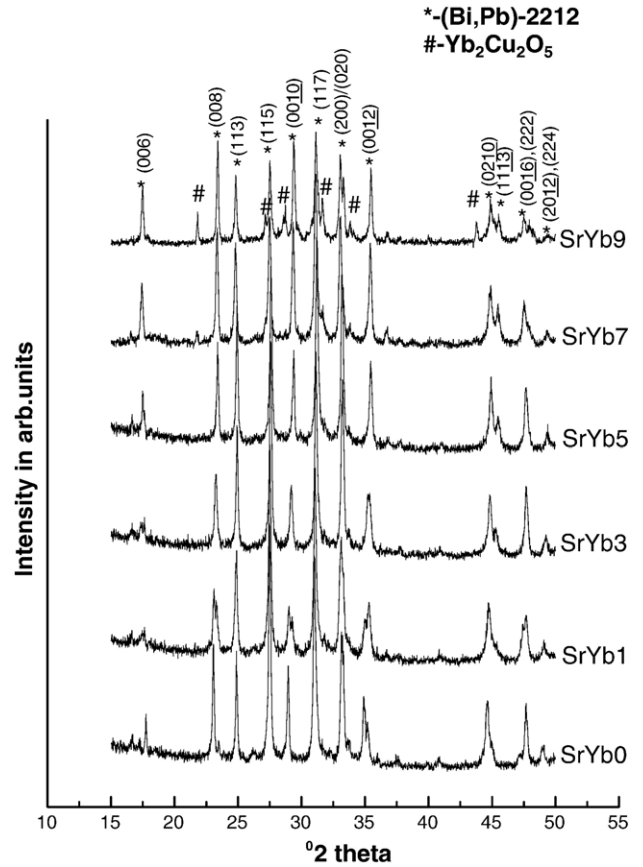

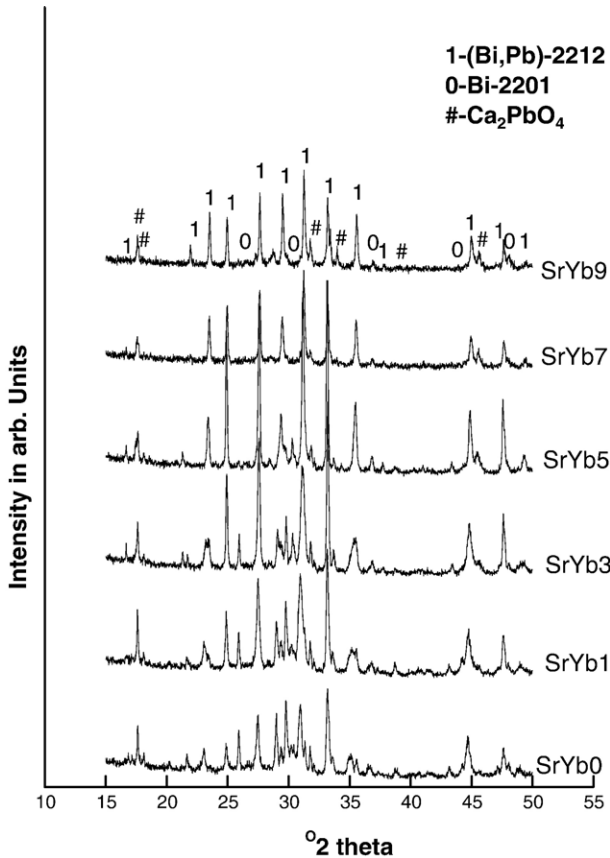Fig. 2. XRD patterns of the samples after the final stage sintering.

database. The densities of the pellets before and after sintering were calculated by measuring the mass and dimensions of the pellets. The T_C and J_C (64 K) were measured using four probe
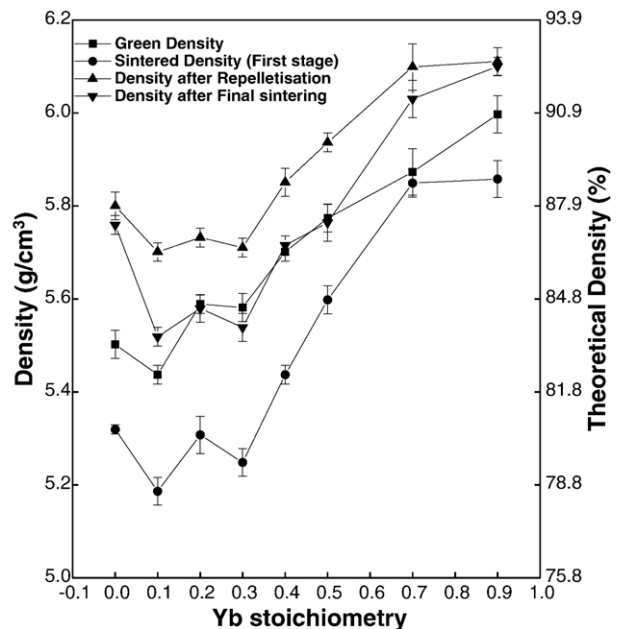

Fig. 1. XRD patterns of the samples after calcination at 820 °C/20 h.

Fig. 3. Density variation of the samples after different stages of heat treatment.

method with 1 μV/cm criterion using a Keithley nanovoltmeter (model 181), a Keithley constant current source (model 220)/an Aplab current source (model 9711P) and a Lakeshore temperature controller (model 340). Electrical contacts were made using highly conducting silver paste applied to the pellet and subsequently cured at 600 °C for 1 h. Microstructural examination of the samples was done using SEM (JEOL JSM 5000LV).

The samples will be hereafter denoted as SrYb0, SrYb1, SrYb2, SrYb3, SrYb4, SrYb5, SrYb7, SrYb9 with Yb content in $Bi_{1.7}Pb_{0.4}Sr_{2-x}Yb_xCa_{1.1}Cu_{2.1}O_y$; where $x=0$, 0.1, 0.2, 0.3, 0.4, 0.5, 0.7, 0.9 respectively.

3. Results and discussion

Fig. 1 shows the XRD patterns of the samples after the second stage calcinations at 820 °C for 20 h. The major phases detected are (Bi, Pb)-2212, Bi-2201. Ca_2PbO_4 is also detected in small amounts in all the samples. Comparing the peak intensities it can be seen that the volume fraction of Bi-2201 decreases and (Bi, Pb)-2212 increases with increasing Yb content. This shows that Yb substitution favours the formation of (Bi, Pb)-2212. Fig. 2 shows the XRD patterns of the samples after final stage of sintering. (Bi, Pb)-2212 is the only phase detected up to an Yb stoichiometry of 0.5 (SrYb5) and there are no peaks of impurity phases, which is in agreement with the previous studies in the case of Ca site substitution and addition of rare earth elements [15,23–25]. In samples SrYb7 and SrYb9 small quantities of $Yb_2Cu_2O_5$ is detected as a secondary phase.

Fig. 3 shows the variation of the density of the samples at different stages of processing. The density values as percentages of the theoretical density of Bi-2212 (6.6 g/cm^3) are shown on the right axis of the figure. After the first stage heat treatment the sintered densities of the samples are less than the corresponding densities before sintering. After final stage of sintering the densities
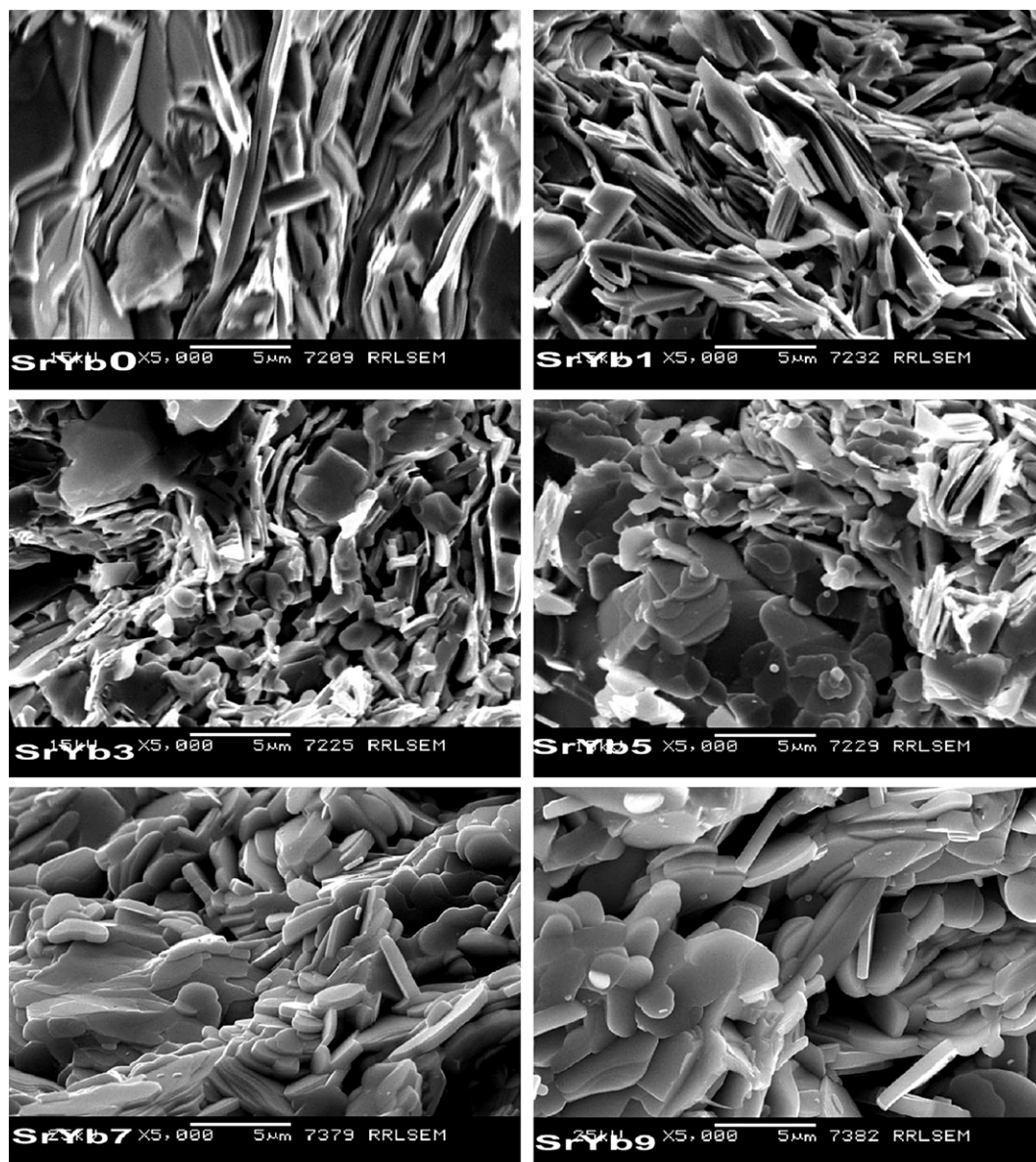

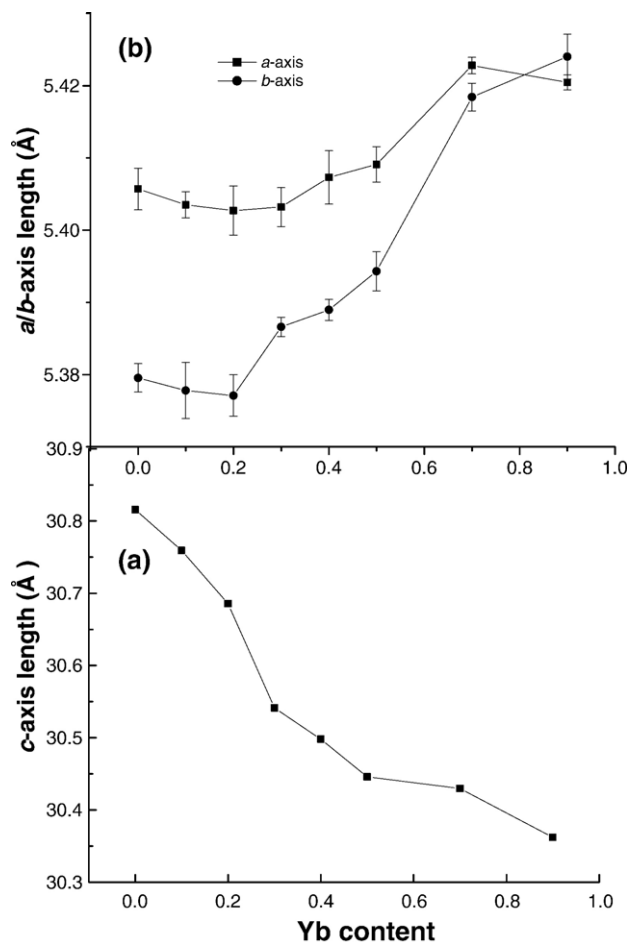Fig. 4. SEM micrographs of the samples taken in the back scattered mode.

Fig. 5. Variation of lattice parameters as a function of Yb substitution.

of all samples except that of the pure sample are found to be less than the density prior to sintering. This is usually referred to as 'retrograde densification' and is a characteristic property of the system. Repeated intermediate pressing reduces the retrograde densification. Here one such intermediate pressing has given and the improvement in density is shown in Fig. 3. In all stages SrYb1 shows a reduction in density compared to pure sample. From SrYb2 onwards the density increases.

Fig. 4 shows the SEM microstructure of the samples (SrYb0, SrYb1, SrYb3, SrYb5, SrYb7 and SrYb9) taken in the back scattered mode. The morphology of the grains shows clear and distinct changes with increase in Yb content. Characteristic flaky grains of (Bi, Pb)-2212 are seen in pure as well as SrYb1 samples. At higher Yb levels (SrYb3 andSrYb5), the microstructures show round or square edged secondary phases scattered in the main matrix. Samples SrYb7 and SrYb9 have a still different morphology. These samples are found to have lesser porosity and the grains are more flattened with rounded edge. The increase in the density of the samples with Yb substitution may be due to the higher density of the secondary phases.

The lattice parameter variations with Yb substitution are shown in Fig. 5. The parameter calculations were based on orthorhombic symmetry assumed for (Bi, Pb)-2212. The c-axis length contracts (Fig. 5(a)) with increase in Yb content as reported in many of the papers for rare earth substitution at Ca site [4–6,10,15,22–26]. In the case of a/b-axis (Fig. 5(b)) there is no considerable change up to

sample SrYb2 and above this concentration both a- and b-axis length increases significantly. The significant change in the lattice parameters with change in Yb doping level implies that Yb enters into the crystal structure. The decrease in c-axis length can be attributed to the fact that the Yb doping leads to an increase in oxygen content in the structure. The excess oxygen could be incorporated into Bi–O layers. This induces a contraction of Bi–O layers and causes an increase in the covalancy of Bi–O bonds. Huong et al. [16] reported the increase in the oxygen content and decrease in copper valancy with increase in doping of La at Sr site in Bi-2212. The change of a/b-axis is generally associated with the change in the Cu–O bond length in CuO_2 planes, which controls the dimensions in the basal planes.

Fig. 6 shows the variation of the normalized resistivity of the samples as a function of temperature. Samples SrYb0 to SrYb5 show superconducting properties whereas samples SrYb7 and SrYb9 show semiconducting behavior. The metal–insulator transition is found to occur at the doping level between $x=0.5$ and 0.7. For pure sample a pseudo transition represented by a sudden drop in resistance, but not reaching to zero, occurs near 110 K. This shows the existence of high T_C phase (Bi-2223) in very small percentages, but the presence of such a phase is not detected in the XRD. As the Yb content increases, the normal state resistivity of the samples also increases (Fig. 7). This shows that the amount of charge carriers decreases with increase in Yb substitution. Earlier reports on Ca site substitution of rare earths [4,11–16] suggest that the conduction at low temperature for $x > 0.55$ is governed by a 2DVRH (Two dimensional Variable-range-hoping) mechanism, whereas for $x=0.55$ a cross over from 2DVRH to 3DVRH occurs, due to the localization of electronic state near the Fermi level. Similar type of changes may be taking place in Sr site substitution also.

Fig. 8 shows the variation of $T_{C\text{-onset}}$ as a function of Yb stoichiometry of the superconducting samples (up to $x=0.5$). The $T_{C\text{-onset}}$ and $T_{C\text{-zero}}$ increases with increase in Yb doping and $T_{C\text{-onset}}$ increases up to 95 K for the sample SrYb3, then it gradually decreases. $\Delta T_C (T_{C\text{-onset}} - T_{C\text{-zero}})$ is minimum for pure sample and higher for doped samples, the highest being for SrYb1 (16.21 K) and decreases up to SrYb3 and then broadens (Table 1). The higher ΔT_C observed for the Yb substituted samples is due to the phase inhomogeneities involving a percolation process between super-conducting region and insulating islands as explained by Muroi and Street [27]. Table 1 also gives the critical current densities of different Yb substituted samples. SrYb2 sample shows the maximum J_C of 1316 A/cm^2 at 64 K, while the pure sample shows a J_C of 101 A/cm^2, i.e. more than thirteen times that of pure sample. Even though SrYb3 shows the maximum T_C, its J_C is less than SrYb2. This may be due to the increased porosity (see Fig. 4) of SrYb3 compared to SrYb2. From SrYb4 onwards J_C values also decreases. These results show that the enhanced critical current density due to the doping can not be attributed to any improvement in the microstructure or the phase purity, because pure sample exhibits a superior microstructure with better phase purity compared to all the Yb substituted samples.

The enhancement in T_C and J_C is related to chemical as well as electronic inhomogeneities which are inseparable and the change in charge carrier (hole) concentration in the Cu–O_2 planes. When Yb is substituted for Sr, Sr^{2+} (1.12 Å) ions are replaced by Yb^{3+} (1.008 Å) ions. The observed changes in the lattice parameters of the Yb substituted samples confirm the entry of Yb at the Sr site. Each substitution of Yb^{3+} for Sr^{2+} fills one hole and a decrease in hole concentration on these planes causes changes in the carrier concentration and can lead to inhomogeneities of the charge reservoir layers.
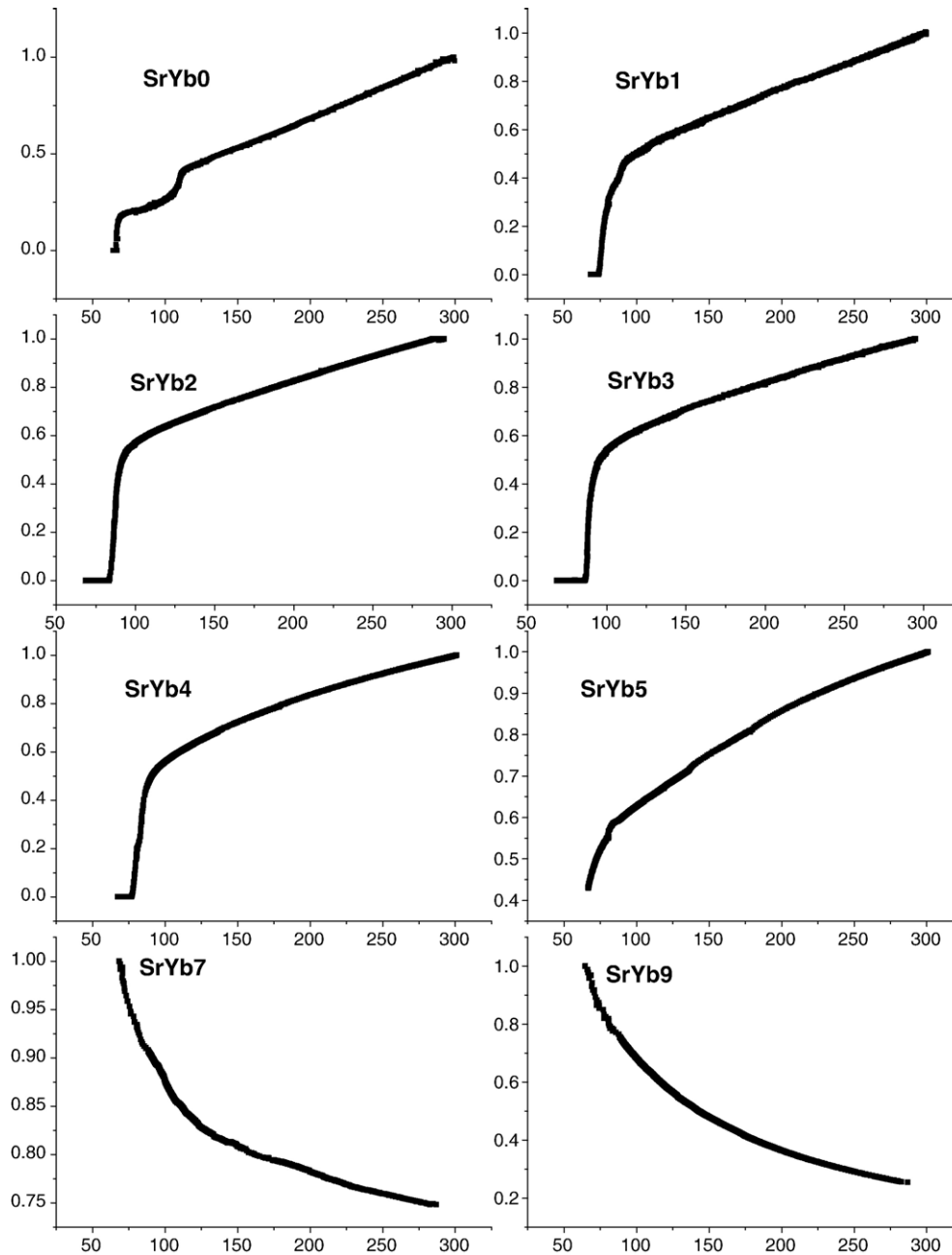
Fig. 6. Variation of the normalized resistivity of the samples as a function of temperature.

Eisaki et al. [2] reported that partial substitution of Sr by rare earths in Bi-2201 results an increase in T_C with decreasing ionic radius mismatch in the case of single crystals. In Bi-2212 also Sr site disorder can be minimized by making disorder at Ca site. But the increase of T_C with substitution of Sr by Yb in (Bi, Pb)-2212 shows that direct substitution at Sr site also can minimize ionic radius mismatch and corresponding increase in T_C. Guptha and Guptha [28] reported that the hole carrier density for pure Bi-2212 is 0.37 hole/Cu–O_2, which is overdoped. For SrYb2 samples the substitution of Yb for Sr may brings the hole density to the optimum value which is estimated to be in the range of 0.2–0.3 hole/Cu–O_2. Inhomogeneities in the structure or secondary phases may create nanoscale flux pinning centres which can also increase transport J_C. The XRD patterns of the samples with higher level of doping and the SEM pictures also give the evidence of secondary phases. When the secondary phase volume increases in the sample, the superconducting properties decrease. Buzea and Yamashitra [29] give a theoretical explanation that the T_C variation with doping concentration (x) depends on the ratio of the superconducting volume and total volume and becomes maximum at a particular value of x and then decreases.

4. Conclusion

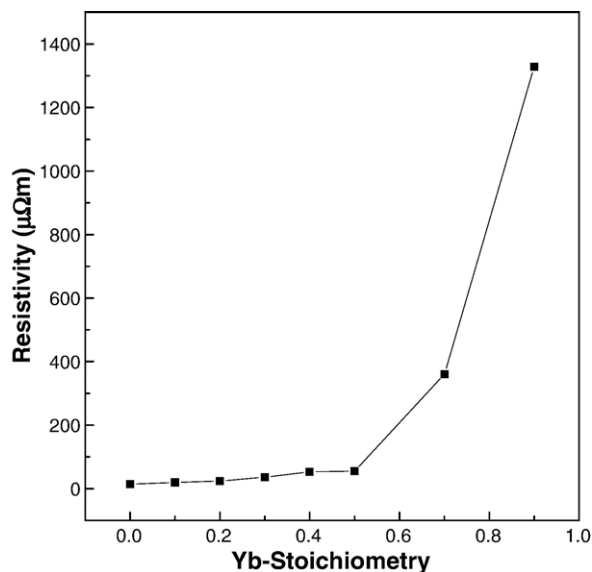This work presents the experimental results of substitution of Yb at the cationic site Sr in the system (Bi, Pb)-2212.

Fig. 7. Variation of normal state resistivity (at 300 K) with Yb stoichiometry.

Table 1
$\Delta T_C (T_{C\text{-onset}} - T_{C\text{-zero}})$ and J_C values of the samples

Yb stoichiometry	$\Delta T_C (T_{C\text{-onset}} - T_{C\text{-zero}})$ (K)	J_C at 64 K (A/cm^2)
0	3.28	101
0.1	16.21	650
0.2	10.33	1316
0.3	8.33	612
0.4	15.00	164
0.5	$T_{C\text{-Zero}}$ below 64 K	–
0.7	Not a superconductor	–
0.9	Not a superconductor	–

secondary phase formation by the substitution of Yb at higher levels also affects the properties of the system.

The phase evolution, microstructure, electrical and super-conducting properties of the system have been studied. The results show that Yb atom enters into the crystal structure. The T_C and J_C are significantly enhanced for optimum concentration of Yb. The maximum T_C is obtained for the sample with $x=0.3$ and J_C for the sample with $x=0.2$, in the stoichiometry $Bi_{1.7}Pb_{0.4}Sr_{2-x}Yb_xCa_{1.1}Cu_{2.1}O_y$. In between the values $0.5<x<0.7$ a metal–insulator transition occurs. At higher doping levels additional secondary phases are observed in the XRD analysis. The changes in the electrical and superconducting properties are due to the chemical as well as electronic inhomogeneities in the structure due to substitution and changes in charge carrier concentration. The
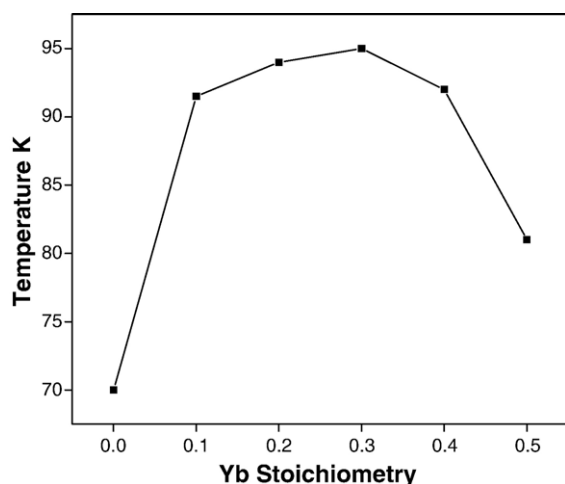
References

[1] J.M. Tarascon, P. Barboux, G.W. Hull, R. Ramesh, L.H. Greene, M. Grioud, M.S. Hedge, W.R. McKinnon, Phys. Rev., B 38 (1989) 4316.
[2] H. Eisaki, N. Kaneko, D. Feng, L. Feng, A. Damascelli, P.K. Mang, K.M. Shen, Z.X. Shen, M. Greven, Phys. Rev., B 69 (2004) 064512.
[3] K. Fujita, T. Noda, K.M. Kojima, H. Eisaki, S. Uchida, Phys. Rev. Lett. 95 (2005) 097006.
[4] P. Mandal, A. Podder, B. Ghosh, P. Choudhary, Phys. Rev., B 43 (1991) 13102.
[5] C.A.M. dos Santos, S. Mochlecke, Y.S. Kopelevich, A.J. Machado, Physica C 390 (2003) 21.
[6] A.Y. Iiyusheehkin, Y. Yamashita, L. Boskorie, I.D. Mackinnon, Super-cond. Sci. Technol. 17 (2004) 1201.
[7] R. Yoshizaki, J. Fujikami, M. Akamatsu, H. Ikda, Supercond. Sci. Technol. 4 S (1991) 421.
[8] P. Somasundaram, R. Vijayaraghavan, R. Nagarajan, R. Seshadri, A.M. Umarji, C.N.R. Rao, Appl. Phys. Lett. 56 (1990) 487.
[9] B. Jayaram, P.C. Lamchester, M. Weller, Phys. Rev., B 43 (1991) 5444.
[10] Y. Gao, P. Pernambuco-Wise, J.E. Crow, J. O'Reilly, N. Spenser, H. Chen, R.E. Salomon, Phys. Rev., B 45 (1992) 7436.
[11] V.P.S. Awana, S.K. Agarawal, A.V. Narlikar, M.P. Das, Phys. Rev., B 48 (1993) 1211.
[12] V.P.S. Awana, S.K. Agarawal, R. Ray, S. Guptha, A.V. Narlikar, Physica C 43 (1992) 1991.
[13] Q. Quitmann, B. Beskhoten, R.J. Kelly, G. Giintherodt, M. Onellion, Phys. Rev., B 51 (1995) 11647.
[14] D. Prabhakaran, C. Subramanian, Physica C 291 (1997) 73.
[15] M. Sangeetha, M. Nagabhushanon, V. Haribabu, F. Beniere, O. Pena, Mater. Sci. Eng., B 58 (1999) 258.
[16] C. Nguyen-van Huong, C. Hinnen, J.M. Siffre, J. Mater. Sci. 32 (1997) 1725.
[17] H. Fuji, H. Kumakura, K. Togano, Physica C 355 (2001) 111.
[18] P. Murugakoothan, R. Jayavel, S.R. Venkatswara Rao, et al., Supercond. Sci. Technol. 7 (1994) 367.
[19] H. Fujii, Y. Hishinuma, H. Kitaguchi, H. Kumakura, K. Togano, Physica C 331 (2000) 79.
[20] T. Motohashi, Y. Nakayama, T. Fujita, K. Kitazawa, J. Shimoyama, K. Kishio, Phys. Rev., B 59 (1999) 14080.
[21] W.D. Wu, A. Keren, L.P. Le, B.J. Sternlieb, G.M. Luke, Y.J. Uemura, Phys. Rev., B 47 (1993) 8172.

Fig. 8. Variation of $T_{C\text{-onset}}$ with Yb stoichiometry.

[22] I. Chong, M. Hiroi, J. Izumi, Y. Shimoyama, Y. Nakayama, K. Kishio, T. Terashima, Y. Bando, M. Takano, Science 276 (1997) 770.

[23] R.P. Aloysius, P. Guruswamy, U. Syamaprasad, Supercond. Sci. Technol. 18 (2005) L1.

[24] A. Biju, R.P. Aloysius, U. Syamaprasad, Supercond. Sci. Technol. 18 (2005) 1454.

[25] V.G. Prabitha, A. Biju, R.G. Abhilash Kumar, P.M. Sarun, R.P. Aloysius, U. Syamaprasad, Physica C 433 (2005) 28.

[26] T. Rentschler, S. Kemmler-sack, M. Hartmann, R.P. Hubenen, P. Kesselar, H. Lichte, Physica C 200 (1992) 287.

[27] M. Muroi, R. Street, Physica C 246 (1995) 347.

[28] R.P. Guptha, M. Guptha, Phys. Rev., B 49 (1994) 13154.

[29] C. Buzea, T. Yamashitra, Physica C 357–360 (2001) 288.